Human Interaction Dynamics for Its Use in Mobile Robotics: Impedance Control for Leader-follower Formation

Daniel Herrera, Flavio Roberti, Marcos Toibero, and Ricardo Carelli, *Senior Member, IEEE*

***Abstract*—A complete characterization of the behavior in human-robot interactions (HRI) includes both: the behavioral dynamics and the control laws that characterize how the behavior is regulated with the perception data. In this way, this work proposes a leader-follower coordinate control based on an impedance control that allows to establish a dynamic relation between social forces and motion error. For this, a scheme is presented to identify the impedance based on fictitious social forces, which are described by distance-based potential fields. As part of the validation procedure, we present an experimental comparison to select the better of two different fictitious force structures. The criteria are determined by two qualities: least impedance errors during the validation procedure and least parameter variance during the recursive estimation procedure. Finally, with the best fictitious force and its identified impedance, an impedance control is designed for a mobile robot Pioneer 3AT, which is programmed to follow a human in a structured scenario. According to results, and under the hypothesis that moving like humans will be acceptable by humans, it is believed that the proposed control improves the social acceptance of the robot for this kind of interaction.**

***Index Terms*—Human modeling, human-machine interaction, impedance control, robot dynamics, social robotics.**

I. Introduction

ACCORDING to the proxemic studies developed by [1], humans respect social zones during different kind of interactions, i.e., there are distances to describe intimate and social spaces depending on the task, the situation, and even on cultural or personal preferences. When a robot follows a human as part of a formation, it is supposed that it must also respect these social zones to improve its social acceptance [2]. For example, [3] discusses different types of personal space for humans according to the situation. The authors assume an egg-shaped personal space for a human in motion, due to the safety assumption that a human should have a long and clear space while walking, thus assuming a potential field with a longer forward axis proportional to the human walking velocity. Scandolo *et al.* use the personal space in their social cost map model for socially acceptable path simulation [4]. In a similar way, Guzzi *et al.* incorporate a potential field that modifies dynamically its dimensions according to the relative distance with the human to avoid an occlusion event or "deadlocks" [5]. In [6] a human-friendly navigation is proposed, where the concept of personal space or "hidden space" is used to prevent uncomfortable feelings when humans plan to avoid or interact with a robot. It is based on human motion and behavior analysis over preliminary experiments, especially face orientation and overlapping personal space.

Even if it seems quite easy to respect these zones like solid barriers, it results inevitably in their meddling when two individuals are interacting and moving. In this way, the comfort of the individual is not only guaranteed through the avoidance of these social zones, but also the dynamics during the meddling events, i.e., they give a natural, smooth and damped motion by considering these as flexible potential zones. Therefore, an impedance, experimentally obtained, should be identified and validated before being used during human-robot interactions. Even when this fact has not been considered in robotics to improve the social acceptance during interactions, in cognitive sciences it has made some contributions to understand the human locomotion behavior during interactions from a dynamics perspective [7], [8].

Defining a human behavior during interactions allows to better characterize robotic motions during human-robot interactions. This assumption stems from the hypothesis that the similarity of the motions improves its social acceptance [9]. This fact should not be confused with the collective behavior of human crowds [10], where the individual dynamics are not relevant.

The dynamic relation that exists between an interaction force and the motion error is usually defined as impedance in robotics. The impedance allows to give specific dynamic qualities to the robotic motions [11]. For example, in [12] an impedance control of a robotic manipulator is presented in a human-robot cooperative task system, where emphasis is made in the stability analysis. Similarly, in [13] a variable impedance control is proposed to include a stiffness coefficient for human-robot cooperation. In addition, within the context of teleoperation, this concept has been taken to improve the transparency by using an online variable impedance control as a natural sensor of human intention [14]. Likewise, when a human operator guides the robot through direct physical

Manuscript received May 31, 2016; accepted August 31, 2016. Recommended by Associate Editor Wei He. *(Corresponding author: Daniel Herrera.)*

Citation: D. Herrera, F. Roberti, M. Toibero, and R. Carelli, "Human interaction dynamics for its use in mobile robotics: Impedance control for leader-follower formation," *IEEE/CAA J. of Autom. Sinica*, vol. 4, no. 4, pp. 696−703, Oct. 2017.

The Authors are all with the Instituto de Automática Universidad Nacional de San Juan-CONICET, Av. Libertador Oeste 1109, San Juan, Argentina (e-mail: dherrera@inaut.unsj.edu.ar; froberti@inaut.unsj.edu.ar; mtoibero@inaut.unsj.edu.ar; rcarelli@inaut.unsj.edu.ar).

Color versions of one or more of the figures in this paper are available online at http://ieeexplore.ieee.org.

Digital Object Identifier 10.1109/JAS.2017.7510631

interaction, it is desirable to have a compliant behavior at the end effector according to a decoupled impedance dynamics [15]. The aforementioned works consider a real force during the interaction, i.e., force feedback through force sensors. The concept of impedance with fictitious forces has also been used to modify the desired velocity of robots, thus deviating the desired robot trajectory to avoid obstacles by considering a desired impedance characteristic [16]−[18]. With this purpose, this paper proposes to describe the human-robot interaction through fictitious potential fields with impedance characteristics, where its flexible nature is determined by the inertial, damping and spring effects of an impedance experimentally identified in a human-human interaction (specifically, a human that follows another one). Later, an impedance control is designed for incorporating this dynamic effect during a human-robot interaction by considering a mobile robot Pioneer 3AT platform.

In Section II, the fictitious forces to be used as social repulsive zones are presented. These forces will be tested and compared to improve the identification of an impedance as defined in Section III. Later, in Section IV, a dynamic control is designed based on feedback linearization and impedance control to incorporate the desired dynamics into the human-robot interactions. In Section V, the experimental results obtained with a mobile robot Pioneer 3AT, are presented. As part of this, an identification stage intended to define the fictitious force, the desired impedance and the dynamical parameters of the robot is included. Finally in Section VI, the conclusions of the work are presented.

II. Fictitious Forces

Based on the representations of fictitious forces given by the literature [16], [19], let us define two general fictitious force structures to describe the social repulsion between individuals. The first one corresponds to piecewise Gaussian functions defined as

$$f_1^{(\mathrm{n})}(t) = \begin{cases} a\dfrac{\left(e^{-\frac{d^n(t)}{d_{\max}}} - e^{-d_{\max}^{n-1}}\right)}{1 - e^{-d_{\max}^{n-1}}}, & \text{if } d(t) < d_{\max} \\ 0, & \text{if } d(t) \geq d_{\max} \end{cases} \tag{1}$$

and the second one corresponds to polynomial functions

$$f_2^{(\mathrm{n})}(t) = \begin{cases} a\left(1 - \left(\dfrac{d(t)}{d_{\max}}\right)^n\right), & \text{if } d(t) < d_{\max} \\ 0, & \text{if } d(t) \geq d_{\max} \end{cases} \tag{2}$$

where $d(t)$ is the distance between individuals at each time instant; $d_{\max}$ the maximal distance of action of the force; a is maximal value of the force, and, $n \in \mathbb{N}$ is the order of the functions.

As previously defined, these functions are continuous and piece-wise defined, and, allow to well establish the limits of action of the fictitious force. These general functions are used in the following sections to define the best one for characterizing an impedance effect.

III. Impedance With Fictitious Forces

The concept of impedance control aims at establishing the dynamic regulation between the motion and the interacting force of the robot with the environment. Physical forces are considered when trying to regulate the mechanical interaction of a robot by using information from force sensors. However, when a non-contact regulation is preferred, fictitious forces are used instead, i.e., a virtual interaction. The linear impedance can be expressed as [16],

$$f(t) = Z(p)\tilde{x}(t) \tag{3}$$

where $p = d/dt$ is the time derivative operator, $f(t)$ is the interacting force of the robot with the environment, $\tilde{x}$ represents the robot motion error in relation to the specified trajectory, and, $Z(p) := Ip^2 + Bp + K$ is the impedance function.

Concerning the human-human interaction context, it is considered that the impedance defines the interaction dynamics itself when a human follows another one, i.e., the linear impedance captures the inertial, damping and spring effects of the human relative motion. On this account, the impedance is identified as follows. By expressing (3) as a parametric model

$$f(t) = \begin{bmatrix} \ddot{\tilde{x}}(t) & \dot{\tilde{x}}(t) & \tilde{x}(t) \end{bmatrix} \begin{bmatrix} I \\ B \\ K \end{bmatrix} \tag{4}$$

then it results in a model with the $\boldsymbol{Y} = \boldsymbol{T}\Theta$ form, which is identified in the following sections by considering a recursive least squares algorithm [20]. In order to estimate the parameters as previously presented, it is necessary to consider a leader relative framework. In this way, the velocity and acceleration of the human follower are given by

$$\nu_{S/L}(t) = \nu_S(t) - \nu_L(t), \quad a_{S/L}(t) = a_S(t) - a_L(t)$$

where $\{\nu_S, \nu_L\}$ are the velocities of the leader and the follower, and $\{a_S, a_L\}$ their accelerations, respectively. This fact makes that the potential field of the human leader acts like a static potential field, as traditionally has been considered.

Additionally, to improve the identification let us consider only the data when $d(t) < d_{\max}$, i.e., when the fictitious force has a non-zero value and a meddling event in the social space is occurring. In this way, let us define a subspace $\mathbb{L} = \{t^* | d(t^*) < d_{\max}\}$. In consequence the motion errors are defined as

$$\tilde{x} := d_d - d(t^*), \quad \dot{\tilde{x}} := \nu_{S/L}(t^*), \quad \ddot{\tilde{x}} := a_{S/L}(t^*)$$

where $d(t)$ is the distance between leader and follower during the experiment, $d_d := \mathrm{mean}(d(t))$ is considered as the desired distance to be followed, which also defines the action range of the fictitious forces, i.e., $d_{\max} := d_d$.

In order to measure such variables, a one-dimension following during the human-human experiment is considered. Concerning practical issues, this fact guarantees that the motion errors are correctly chosen, and, consequently, the impedance will be correctly defined.

Additionally, to define the best structure for the fictitious force $f(t)$ and to obtain experimental results, the criteria are

determined by two qualities: least impedance errors during the validation procedure and least parameter variance during the recursive estimation procedure. Therefore, in Section V-B, an experimental comparison is presented by considering some fictitious force candidates and identification results. This allows validating both the impedance parameters that were identified, and, the fictitious interaction force model that has been chosen.

IV. Dynamic Motion Control for Human Following

A. Robot Dynamic Model

Consider that the dynamic model for a differential drive mobile robot is defined by [21]

$$\begin{bmatrix}\dot{x}_r\\ \dot{y}_r\\ \dot{\psi}_r\\ \dot{\nu}_r\\ \dot{\omega}_r\end{bmatrix} = \begin{bmatrix}\nu_r\cos\psi_r - a\omega_r\sin\psi_r\\ \nu_r\sin\psi_r + a\omega_r\cos\psi_r\\ \omega_r\\ \dfrac{\theta_3^{(\mathrm{r})}}{\theta_1^{(\mathrm{r})}}\omega_r^2 - \dfrac{\theta_4^{(\mathrm{r})}}{\theta_1^{(\mathrm{r})}}\nu_r\\ -\dfrac{\theta_5^{(\mathrm{r})}}{\theta_2^{(\mathrm{r})}}\nu_r\omega_r - \dfrac{\theta_6^{(\mathrm{r})}}{\theta_2^{(\mathrm{r})}}\omega_r\end{bmatrix} + \begin{bmatrix}0 & 0\\ 0 & 0\\ 0 & 0\\ \dfrac{1}{\theta_1^{(\mathrm{r})}} & 0\\ 0 & \dfrac{1}{\theta_2^{(\mathrm{r})}}\end{bmatrix}\begin{bmatrix}\nu_d\\ \omega_d\end{bmatrix} \quad (5)$$

where $\Theta_r = \{\theta_1^{(\mathrm{r})}, \theta_2^{(\mathrm{r})}, \theta_3^{(\mathrm{r})}, \theta_4^{(\mathrm{r})}, \theta_5^{(\mathrm{r})}, \theta_6^{(\mathrm{r})}\}$ are the parameters of the robot model, (x_r, y_r, ψ_r) its posture, $\{\nu_r, \omega_r\}$ its linear and angular velocity, and, $\{\nu_d, \omega_d\}$ its linear and angular velocity references.

B. Feedback Linearization Control

If it is considered that the control objective is to keep a relative position with respect to the human leader, then the output vector is defined by the robot position

$$\boldsymbol{x}_r = \begin{bmatrix}x_r\\ y_r\end{bmatrix}.$$

Additionally, by considering the robot model defined in (5), the first and second time derivative of the output can be expressed as

$$\dot{\boldsymbol{x}}_r = \begin{bmatrix}\dot{x}_r\\ \dot{y}_r\end{bmatrix} = Jv_r, \qquad \ddot{\boldsymbol{x}}_r = \boldsymbol{q} + J\left(\boldsymbol{g} + H\boldsymbol{u}_d\right) \quad (6)$$

with $\boldsymbol{v}_r = [\nu_r, \omega_r]^T$ the velocity vector of the robot, $\boldsymbol{u}_d = [\nu_d, \omega_d]^T$ its velocity references, and,

$$J := \begin{bmatrix}\cos\psi_r & -a\sin\psi_r\\ \sin\psi_r & a\cos\psi_r\end{bmatrix},$$

$$\boldsymbol{q} := \begin{bmatrix}-u_r w_r\sin\psi_r - aw_r^2\cos\psi_r\\ u_r w_r\cos\psi_r - aw_r^2\sin\psi_r\end{bmatrix},$$

$$\boldsymbol{g} := \begin{bmatrix}\dfrac{\theta_3^{(\mathrm{r})}}{\theta_1^{(\mathrm{r})}}w_r^2 - \dfrac{\theta_4^{(\mathrm{r})}}{\theta_1^{(\mathrm{r})}}u_r\\ -\dfrac{\theta_5^{(\mathrm{r})}}{\theta_2^{(\mathrm{r})}}u_r w_r - \dfrac{\theta_6^{(\mathrm{r})}}{\theta_2^{(\mathrm{r})}}w_r\end{bmatrix}, \; H := \begin{bmatrix}\dfrac{1}{\theta_1^{(\mathrm{r})}} & 0\\ 0 & \dfrac{1}{\theta_2^{(\mathrm{r})}}\end{bmatrix}.$$

If the following control of feedback linearization is defined in (6)

$$\boldsymbol{u}_d := H^{-1}\left[J^{-1}\left(\boldsymbol{v} - \boldsymbol{q}\right) - \boldsymbol{g}\right]. \quad (7)$$

then the resultant system is an input-output linear system with the form $\ddot{\boldsymbol{x}}_r = \boldsymbol{v}$.

In this way, it remains to define the auxiliary input $\boldsymbol{v}$, which acts like an external loop as shown in Fig. 2. For this, an impedance control is proposed to establish a dynamic relation between the fictitious force and the motion error during the following of the human leader, as detailed below.

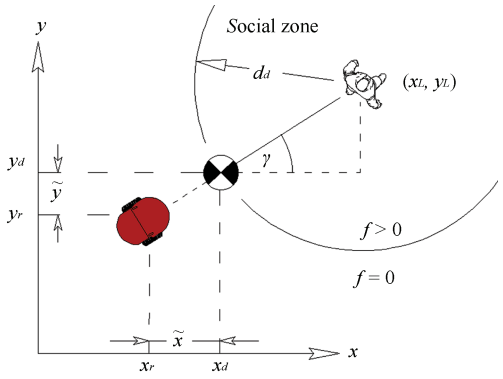

Fig. 1. Leader-follower system.

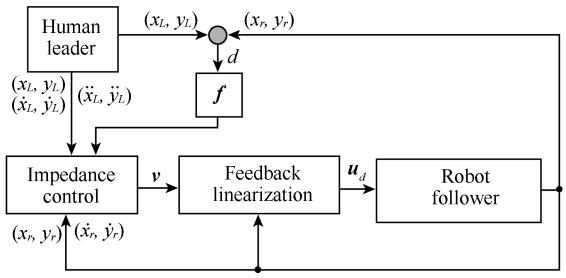

Fig. 2. Scheme of control.

C. Impedance Control

When a robot escorts a human, it meddles inherently in the social zone of the human. During this event, the robot is aimed to guarantee social dynamics that promote its comfort and motivate the interaction. For this, it is proposed to characterize these dynamics through an impedance control.

Let us define the motion error on each coordinate axis $\tilde{\boldsymbol{x}} = [x_d - x_r, y_d - y_r]^T$ and the desired impedance

$$\boldsymbol{f}_{\text{desired}}(t) = \left(Ip^2 + Bp + K\right)\tilde{\boldsymbol{x}}(t) \quad (8)$$

where $I = \mathrm{diag}(I, I)$ is the inertia matrix, $B = \mathrm{diag}(B, B)$ the damping matrix, and, $K = \mathrm{diag}(K, K)$ the elasticity matrix, with $\{I, B, K\}$ identified as presented in Section III. Additionally $x_d := x_L - d_d\cos\gamma$, $y_d := y_L - d_d\sin\gamma$, where, $(x_L, y_L), (x_r, y_r)$ are the global position of the human leader and the robot follower respectively, and, γ is their relative orientation (see Fig. 1).

To define the interaction social force, the potential is regarded to be centered at (x_L, y_L), where the magnitude of the fictitious repulsive force is defined by (1) or (2) with direction γ. Therefore, the force components in x, y are decomposed as follows $\boldsymbol{f}_{\text{social}} := [f_j^{(\mathrm{n})}(t)\cos\gamma, f_j^{(\mathrm{n})}(t)\sin\gamma]$, $j = \{1, 2\}$.

Once that the interaction force and the motion error are defined, the auxiliary input $\boldsymbol{v}$ is defined based on an impedance control as below

$$\boldsymbol{v} := \ddot{\boldsymbol{x}}_L + I^{-1}\left(B\dot{\tilde{\boldsymbol{x}}} + K\tilde{\boldsymbol{x}} - \boldsymbol{f}_{\text{social}}\right) \tag{9}$$

where $\dot{\tilde{\boldsymbol{x}}}$ is the time derivative of the motion error, and, $\ddot{\boldsymbol{x}}_L = [\ddot{x}_L, \ddot{y}_L]$ is the acceleration vector of the leader in the global framework. In this way, substituting (9) in (7), the impedance control is defined as

$$\boldsymbol{u}_d := H^{-1}\Big[J^{-1}\Big(\ddot{\boldsymbol{x}}_L + I^{-1}\Big(B\dot{\tilde{\boldsymbol{x}}} + K\tilde{\boldsymbol{x}} - \boldsymbol{f}_{\text{social}}\Big) - \boldsymbol{q}\Big) - \boldsymbol{g}\Big]. \tag{10}$$

V. Experimental Results

A. Experimental Setup

For estimating the parameters of the impedance model (4), it is necessary to take measures of two humans, one following the other, and with this data, be able to estimate the variables involved in the identification. For this, a range sensor LIDAR is located in the world space as shown in Fig. 3. This sensor is capable of taking measures of up to 30 meters, with a 180° scanning angle and 0.5° or 1° resolution.

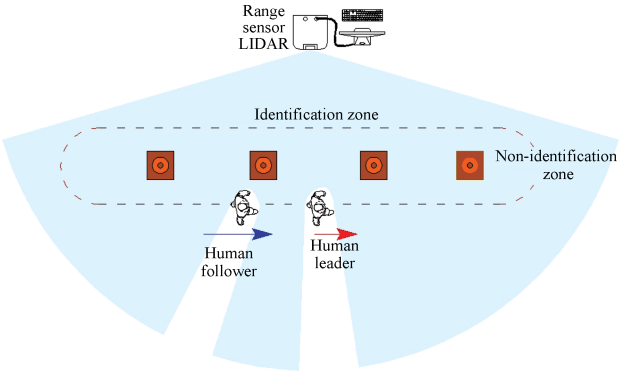

Fig. 3. Experimental scenario.

Thus, the scenario consists of a structured environment that is horizontally scanned by a laser range sensor. Therefore, during the experiment, the scenario is only visited by the two involved participants, who are coming one after the other (see Fig. 4). The collected range points with high distance variations define the meddling of humans in the scenario. These points are classified through an agglomerative hierarchical cluster tree, that is used later to classify in two groups according to its distance correlation.

Fig. 4. Experiment photo sequence.

Once the two groups are established, two characteristic points are defined through the mean point of each cluster. And finally, an α-β filter is used to obtain the positions, orientations and velocities of both participants [21].

B. Identification Stage

1) Impedance Identification: In Fig. 5 the data obtained during the experiment is graphically presented. From this data, the motion error and the values of fictitious force are estimated.

From these, just those values that lie within the "identification zone" of Fig. 3 are considered, because only in such zone the desired dynamic effect can be well characterized. Furthermore, these values are divided into two groups for the identification and validation procedures respectively, as shown in Fig. 5. The data used in the identification procedure is presented in Fig. 6, and corresponding to 540 samples with a sample time of 0.1 second.

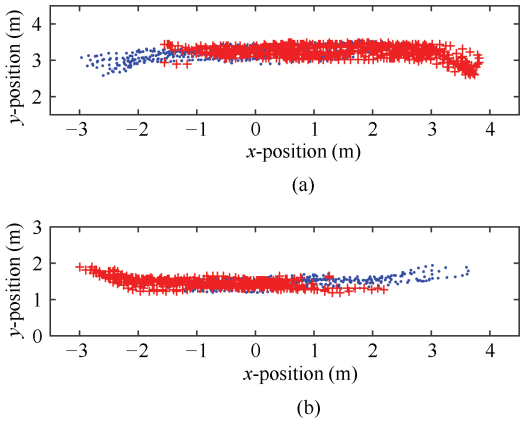

Fig. 5. Overlapped experimental trajectories of the human leader (red sum "+" symbols) and follower (blue points) during the experiment. (a) Data for identification. (a) Data for identification. (b) Data for validation.

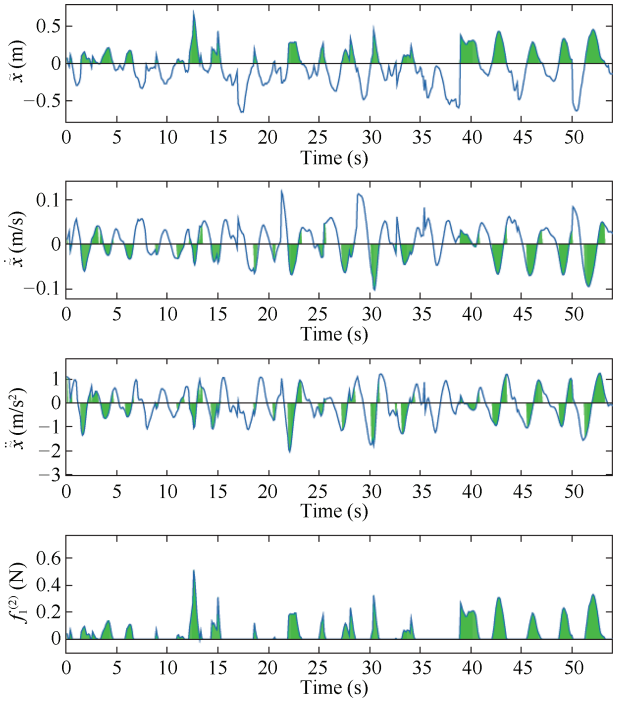

Fig. 6. Experimental estimated variables.

As mentioned, to improve the identification procedure only the data during the periods when $d(t) < d_{\max}$ is used, i.e., $f_j^{(n)} \neq 0$ (see marked zones in Fig. 6). This data is presented randomly until reaching parameters convergence as many times as it is necessary.

This identification procedure is repeated a number of times by considering different fictitious force models, and their results are compared by considering its variance (in convergence state) during the parameters identification procedure, and, by considering the impedance error given by the validation procedure.

The impedance error $\xi(t)$ is calculated as follows

$$\xi(t) = f_j^{(n)} - \left(I_j^{(n)}\ddot{\tilde{x}} + B_j^{(n)}\dot{\tilde{x}} + K_j^{(n)}\tilde{x}\right) \tag{11}$$

where $I_j^{(n)}, B_j^{(n)}, K_j^{(n)}$ are the parameters identified by considering the fictitious force $f_j^{(n)}, j = \{1, 2\}, n \in \mathbb{N}$ during the identification and validation procedure, and, $\{\ddot{\tilde{x}}, \dot{\tilde{x}}, \tilde{x}\}$ is the experimental validation data. For each fictitious force, a maximum value $a = 100$ N and a maximal range $d_{\max} = 1.55$ m are considered. Results are summarized in Table I.

TABLE I
COMPARISON BETWEEN FICTITIOUS FORCE MODELS

Fictitious force	Impedance error		Parameter variance*		
	RMSE	r^{**}	σ_I	σ_B	σ_K
$f_1^{(2)}$	0.2564	0.9998	6.1458×10^{-5}	0.0025	0.0221
$f_1^{(4)}$	0.6664	0.9989	6.8462×10^{-4}	0.0286	0.1875
$f_1^{(10)}$	7.3994	0.9605	0.0236	0.4817	1.4054
$f_2^{(2)}$	1.1008	0.9987	8.3680×10^{-4}	0.0412	0.2081
$f_2^{(4)}$	4.9873	0.9890	0.0117	0.3077	1.0507
$f_2^{(10)}$	18.4340	0.9246	0.1270	2.3268	3.5112

*Variance of the parameters during the identification (last 400 samples).

**Mean correlation coefficients (r).

By analyzing the obtained values in Table I and by considering the aforementioned criteria, the fictitious force $f_1^{(2)}$ is regarded the best one, and its identification and validation results are detailed in Figs. 7 and 8, respectively.

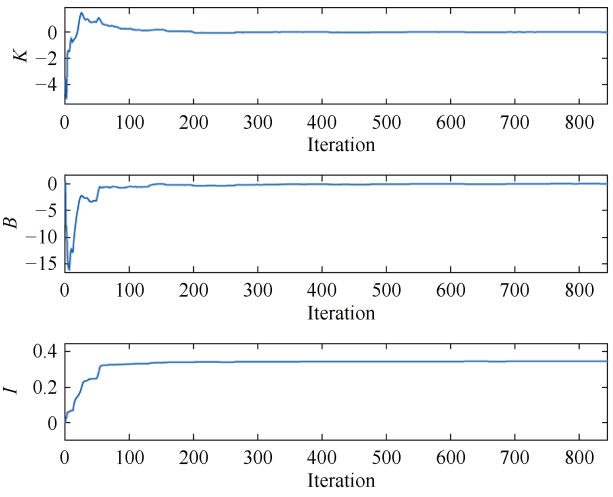

Fig. 7. Recursive least squares identification.

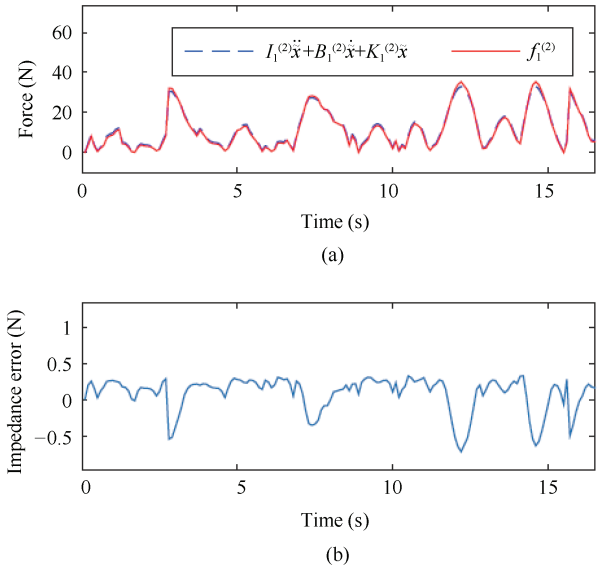

Fig. 8. Experimental validation by considering $f_1^{(2)}$. (a) Impedance (dashed blue line) and fictitious measured force (red line). (b) Impedance error.

Finally, the obtained parameters results are selected to be: $K = 0.01, B = 0.19, I = 0.35$.

2) Identification of the Robotic Platform: In order to obtain experimental results with a control of feedback linearization (7), it is necessary to identify the dynamic model of the robot. This is done by considering a filtered regression model as presented in [22]. The data for the identification and validation procedures are presented in Fig. 9.

The identified parameters of the model (5) for a differential drive model robot Pioneer 3AT (used in the internal control loop) are: $\theta_1^{(r)} = 0.3037$, $\theta_2^{(r)} = 0.2768$, $\theta_3^{(r)} = -0.0004018$, $\theta_4^{(r)} = 0.9835$, $\theta_5^{(r)} = -0.003818$, $\theta_6^{(r)} = 1.0725$.

C. Human-following Control

By considering the aforementioned experimental scenario, it is possible to determine the position of the human and derive the necessary variables to program the proposed control in a global framework (x, y). This information is sent to the mobile robotic platform Pioneer 3AT which incorporates a low-level controller to regulate the linear and angular velocities. Data exchange is done through a server-client connection, which allows to transfer the action commands to the robot and to receive the odometer sensor data of the robot and the involved variables of the human motions of the scanned scenario (see Fig. 10).

In this way, with the parameters identified in Sections V-B1 and V-B2, the previously designed controller (10) for a Pioneer 3AT is programmed. The experiment consists of following a human while he is moving along a quasi-circular trajectory during 715 samples with a sample time of 0.1 seconds.

Note that the escorting is not fixed to the rear position of the human, but it is adjusted dynamically by considering the relative orientation between human and robot (see Fig. 11 or watch a video clip at https://youtu.be/7TdG-kzN3pE). Even though it is an interesting fact to choose the optimal human relative position from a "comfort" sense, this fact is neverthe-

less regarded irrelevant for the present work and it has been only focused on the dynamic aspects of the interaction.

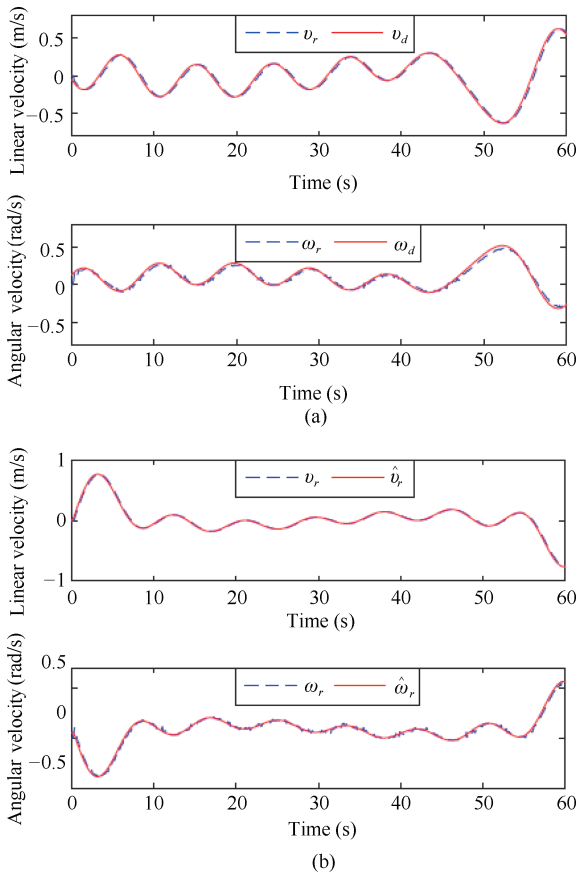

Fig. 9. Experimental Pioneer 3AT data. (a) Reference (red line) and measured velocities (dashed blue line) for identification. (b) Reference (red line) and measured velocities (dashed blue line) for validation.

Fig. 10. Experimental platform.

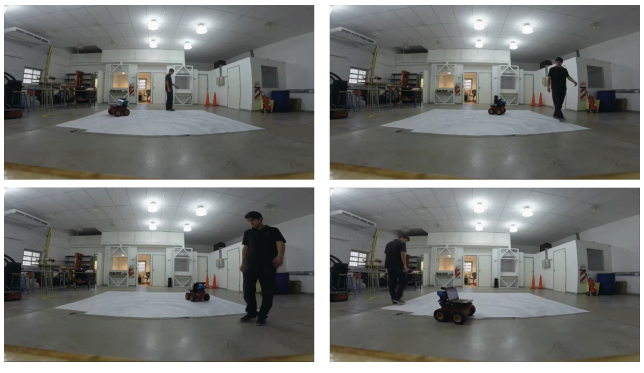

Fig. 11. Experimental photo sequence.

In Fig. 12, a subset of the experimental trajectories is presented, where the fictitious potential fields are represented as well. Additionally, in Fig. 13 the motion errors are shown for each axis, where the events of meddling in the social zone are marked as repulsion forces, i.e., $f_x > 0$ and $f_y > 0$. Traditionally, a motion control is intended to obtain a minimum motion error, however it is not a relevant fact when it is expected to generate specific dynamic behaviors. Consequently, this paper is focused only on validating the impedance that was generated during the robotic task. This way, in Fig. 14, the impedance generated by the robot and the measured fictitious force during the meddling events are compared, where the mean squared errors (RMSE) for each axis result to be $\text{RMSE}_x = 1.3429$ and $\text{RMSE}_y = 0.8966$, and the mean correlation coefficients are $r_x = 0.9882$ and $r_y = 0.9847$. Finally, the impedance errors are presented in Fig. 15. And, in Fig. 16, the control actions $\{\nu_d, \omega_d\}$ and the measured velocities of the mobile robot $\{\nu_r, \omega_r\}$ during the test are shown.

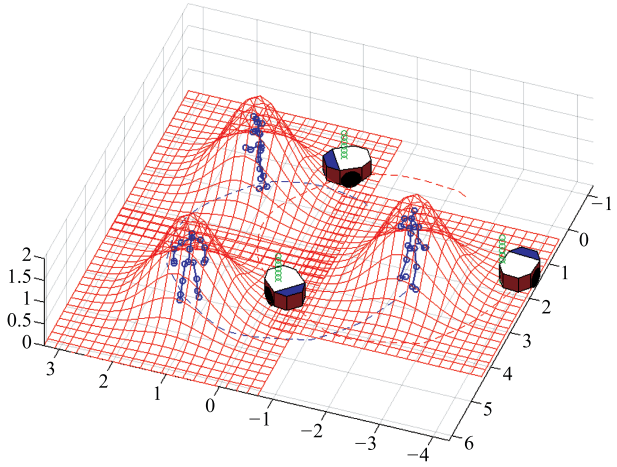

Fig. 12. Subset of the experimental trajectories.

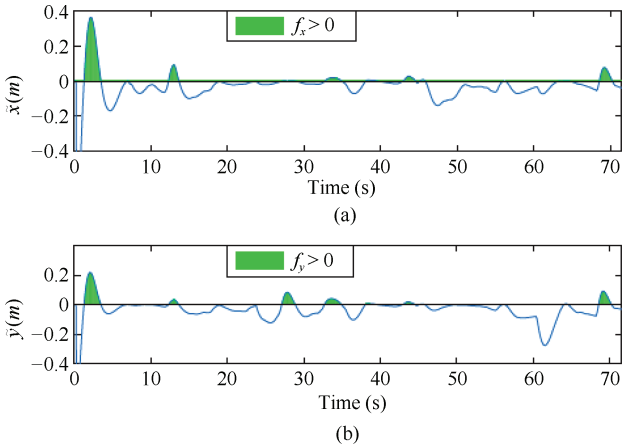

Fig. 13. Motion error. (a) x-axis. (b) y-axis.

VI. Conclusions

This paper has presented the design of a coordinate leader-follower control based on impedance control and feedback linearization. This allows establishing a dynamic relation between the motion error and a fictitious social, force. With

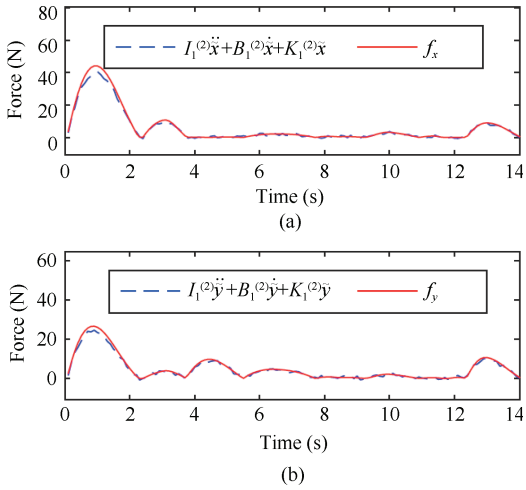

Fig. 14. Impedance (dashed blue line) and interaction force (red line). (a) x-axis. (b) y-axis.

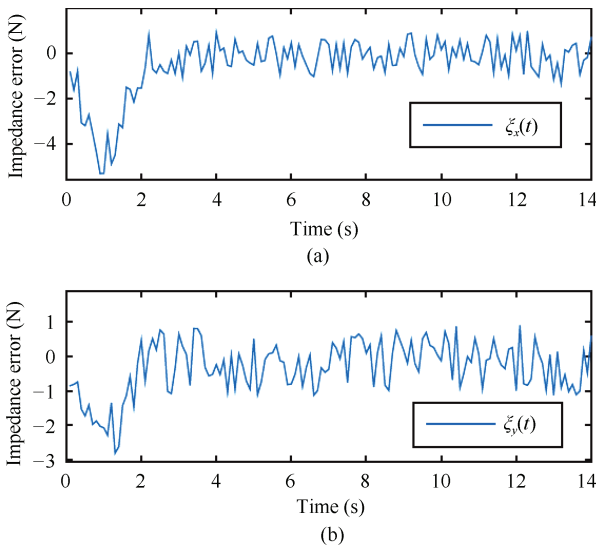

Fig. 15. Impedance errors. (a) x-axis. (b) y-axis.

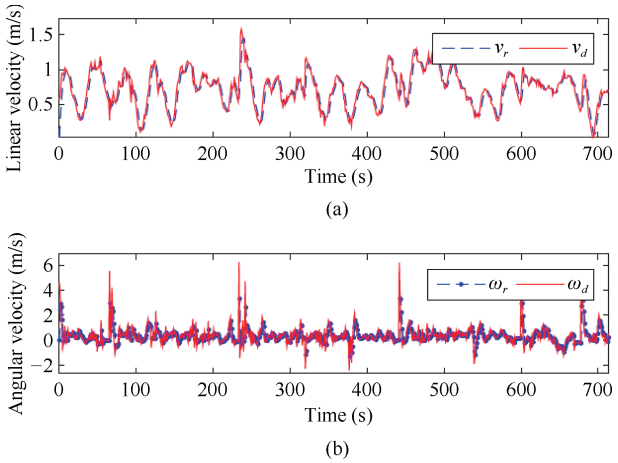

Fig. 16. Measured (blue dashed lines) and reference (red lines) robot velocities. (a) Linear velocity. (b) Angular velocity.

the purpose of better characterizing this behavior for the human-robot interaction, an experimental identification of the inertial, damping and elasticity properties of the impedance in a human-human interaction has been proposed, where several models have been tested to select the appropriate one for the impedance identification. Finally by using the identified parameters in the proposed control, a mobile robot Pioneer 3AT has been programmed to follow a human in a structured scenario that is horizontally scanned by a LIDAR range sensor. The results show that the robot is capable of emulating the previously identified impedance and, consequently, it is believed that the proposed control can improve the social acceptance by being able to imitate this human-human dynamic behavior.

REFERENCES

[1] E. T. Hall, "A system for the notation of proxemic behavior," *Am. Anthropolog.*, vol. 65, no. 5, pp. 1003−1026, Oct. 1963.

[2] J. Rios-Martinez, A. Spalanzani, and C. Laugier, "From proxemics theory to socially-aware navigation: A survey," *Int. J. Soc. Robot.*, vol. 7, no. 2, pp. 137−153, Apr. 2015.

[3] C. P. Lam, C. T. Chou, K. H. Chiang, and L. C. Fu, "Human-centered robot navigation—Towards a harmoniously human-robot coexisting environment," *IEEE Trans. Robot.*, vol. 27, no. 1, pp. 99−112, Feb. 2011.

[4] L. Scandolo and T. Fraichard, "An anthropomorphic navigation scheme for dynamic scenarios," in *Proc. 2011 IEEE Int. Conf. Robotics and Automation*, Shanghai, China, 2011, pp. 809−814.

[5] J. Guzzi, A. Giusti, L. M. Gambardella, G. Theraulaz, and G. A. Di Caro, "Human-friendly robot navigation in dynamic environments," in *Proc. 2013 IEEE Int. Conf. Robotics and Automation*, Karlsruhe, 2013, pp. 423−430.

[6] P. Ratsamee, Y. Mae, K. Ohara, M. Kojima, and T. Arai, "Social navigation model based on human intention analysis using face orientation," in *Proc. 2013 IEEE/RSJ Int. Conf. Intelligent Robots and Systems*, Tokyo, Japan, 2013, pp. 1682−1687.

[7] K. W. Rio, C. K. Rhea, and W. H. Warren, "Follow the leader: Visual control of speed in pedestrian following," *J. Vision*, vol. 14, no. 2, p. 4, Feb. 2014.

[8] G. C. Dachner and W. H. Warren, "Behavioral dynamics of heading alignment in pedestrian following," *Trans. Res. Procedia*, vol. 2, pp. 69−76, Dec. 2014.

[9] T. Kruse, A. K. Pandey, R. Alami, and A. Kirsch, "Human-aware robot navigation: A survey," *Robot. Autonom. Syst.*, vol. 61, no. 12, pp. 1726−1743, Dec. 2013.

[10] D. Helbing and A. Johansson, *Pedestrian, Crowd and Evacuation Dynamics*. New York: Springer, 2009, pp. 6476−6495.

[11] A. Calanca, R. Muradore, and P. Fiorini, "A review of algorithms for compliant control of stiff and fixed-compliance robots," *IEEE/ASME Trans. Mechatron.*, vol. 21, no. 2, pp. 613−624, Apr. 2016.

[12] T. Tsumugiwa, R. Yokogawa, and K. Yoshida, "Stability analysis for impedance control of robot for human-robot cooperative task system," in *Proc. 2004 IEEE/RSJ Int. Conf. Intelligent Robots and Systems*, Sendai, 2004, pp. 3883−3888.

[13] J. Bae, J. Ko, and D. Hong, "Variable impedance control with stiffness for human-robot cooperation system," in *Proc. 15th Int. Conf. Control, Automation and Systems*, Busan, 2015, pp. 1231−1233.

[14] V. Duchaine and C. M. Gosselin, "General model of human-robot cooperation using a novel velocity based variable impedance control," in *Proc. 2nd Joint EuroHaptics Conf., 2007 and Symp. Haptic Interfaces for Virtual Environment and Teleoperator Systems*, Tsukuba, Japan, 2007, pp. 446−451.

[15] F. Ficuciello, L. Villani, and B. Siciliano, "Redundancy resolution in human-robot co-manipulation with cartesian impedance control," in *Experimental Robotics*, M. Ani Hsieh, O. Khatib, and V. Kumar, Eds. Switzerland: Springer International Publishing, 2016, pp. 165−176.

[16] R. Carelli, J. Santos-Victor, F. Roberti, and S. Tosetti, "Direct visual tracking control of remote cellular robots," *Robot. Autonom. Syst.*, vol. 54, no. 10, pp. 805−814, Oct. 2006.

[17] T. Tsuji, H. Akamatsu, and M. Kaneko, "Non-contact impedance control for redundant manipulators using visual information," in *Proc. 1997 IEEE Int. Conf. Robotics and Automation*, Albuquerque, NM, USA, 1997, pp. 2571−2576.

[18] S. Y. Lo, C. A. Cheng, and H. P. Huang, "Virtual impedance control for safe human-robot interaction," *J. Intell. Robot. Syst.*, vol. 82, no. 1, pp. 3−19, Apr. 2016.

[19] D. Helbing and P. Molnár, "Social force model for pedestrian dynamics," *Phys. Rev. E*, vol. 51, no. 5, pp. 4282−4286, May 1995.

[20] W.-C. Yu and N.-Y. Shih, "Bi-loop recursive least squares algorithm with forgetting factors," *IEEE Signal Proc. Lett.*, vol. 13, no. 8, pp. 505−508, Aug. 2006.

[21] P. R. Kalata, "The tracking index: A generalized parameter for α-β and α-β-γ target trackers," *IEEE Trans. Aerosp. Electron. Syst.*, vol. AES-20, no. 2, pp. 174−182, Mar. 1984.

[22] C. De la Cruz and R. Carelli, "Dynamic model based formation control and obstacle avoidance of multi-robot systems," *Robotica*, vol. 26, no. 3, pp. 345−356, May 2008.

Daniel Herrera received the degree in electronic and control engineering from the National Polytechnic School of Ecuador in 2012, where he was also Laboratory Assistant at the Department of Automation and Industrial Control. He obtained the Ph.D. degree in control systems engineering at the Institute of Automatics (INAUT) of the National University of San Juan, Argentina in March 2017. Currently, he is a Postdoctoral Researcher at INAUT. His research interests include human-robot interactions, artificial intelligence and robots modeling.

Flavio Roberti graduated in engineering from the National University of San Juan, Argentina in 2004, and received the Ph. D. degree in control systems engineering from the National University of San Juan, Argentina in 2009. He is currently an Assistant Professor at the National University of San Juan and a Researcher of the National Council for Scientific and Technical Research (CONICET, Argentina). His research interests include robotics, wheeled mobile robots, mobile manipulators, visual servoing and passivity based visual control.

Marcos Toibero received the B. E. degree in electronics engineering from the Technological National University of Argentina, in Paraná, Argentina, in 2002, and the Ph.D. degree in engineering from the San Juan National University, San Juan, Argentina, in 2007. In 2005, he joined the Instituto de Automática (INAUT), in the San Juan National University of Argentina. In 2011, he became a Researcher of the CONICET. His current research interests include robotics control, nonlinear systems, switching systems, robot-human interaction and precision agriculture applications.

Ricardo Carelli graduated in engineering from the National University of San Juan, Argentina, and received the Ph.D. degree in electrical engineering from the National University of Mexico (UNAM). He is a Full Professor at the National University of San Juan and a senior researcher of the National Council for Scientific and Technical Research (CONICET, Argentina). Prof. Carelli is the Director of the Instituto de Automática, National University of San Juan (Argentina). His research interests include in robotics, manufacturing systems, adaptive control and artificial intelligence applied to automatic control. Prof. Carelli is a senior member of IEEE and a member of AADECA-IFAC.